Journal of ELECTRONIC MATERIALS, Vol. 48, No. 4, 2019
https://doi.org/10.1007/s11664-018-6623-9

TOPICAL COLLECTION: INTERNATIONAL CONFERENCE ON THERMOELECTRICS 2018

Improvement of the Thermoelectric Properties of the Perovskite $SrTiO_3$ by Cr-Doping

TAMAL TAHSIN KHAN,[1] IL-HO KIM,[1] and SOON-CHUL UR[1,2]

1.—Department of Materials Science and Engineering and Research Center for Sustainable Eco-Devices and Materials (ReSEM), Korea National University of Transportation, Chungju 27469, Republic of Korea. 2.—e-mail: scur@ut.ac.kr

In recent years, among different thermoelectric materials, $SrTiO_3$ have been receiving great attention due to their greater capacity and conversion between electrical energy and heat energy. The thermoelectric properties of the $SrTiO_3$ can be improved by substitutional doping on different sites (A-site and B-site) in the lattice. In this study, the improvement of the thermoelectric performance of the perovskite $SrTiO_3$ by Cr-doping has been investigated. The doped $SrTiO_3$ with Cr was synthesized by the conventional solid-state reaction method. The electronic transport properties including Seebeck coefficient, electrical conductivity, and thermal transport properties in a moderate temperature regime from 300 to 900 K have been investigated. The large absolute value of the Seebeck coefficient with low thermal conductivity was achieved by Cr-doping. The electrical conductivity was quite low but increased with increasing doping level up to $x = 0.002$ mol, and; hence, the power factor increased with increasing doping level up to $x = 0.002$ mol. The maximum ZT value was observed for $SrTi_{0.998}Cr_{0.002}O_3$ at 773 K by the combination of a high value of the Seebeck coefficient and low thermal conductivity.

Key words: Perovskite oxide, doping, vacuum hot-pressing, electronic properties

INTRODUCTION

Nowadays, the demand for more sustainable energy sources has been increased with increasing population growth. Thermoelectric (TE) materials have the potential as clean and environmentally friendly power sources, which generate power from the waste-heat of different industrial processes, furnaces, and engine exhaust streams that are otherwise lost to the surroundings. The non-renewable energy sources, like fossil fuels, cause negative environmental effects by emitting pollutants such as CO_2 and increased greenhouse gases, which lead to global warming that have a huge impact on the quality of life on the earth. Thermoelectric energy and other renewable energy sources such as wind and hydro-power can reduce these emissions and should be invested in for further research.[1] The major sources of energy might be depleted and the world will fall into a huge energy crisis according to Shafiee and Topal.[2] TE materials, capable of converting waste heat to electric energy from the burning of these fossil fuels, have received extensive interest in recent years.[3–5] The efficiency of the TE materials are characterized by a high thermoelectric figure of merit, $ZT = S^2\sigma T/\kappa$, where S, σ, and $\kappa = \kappa_E + \kappa_L$ are the Seebeck coefficient, electrical conductivity, and thermal conductivity (with electronic and lattice contributions), respectively.

So far, the proposed high performance thermoelectric materials are complex chalcogenides,[6] skutterudites,[7] clathrates,[8] and half-Heusler alloys.[9] All the proposed materials are both chemically and physically unstable at high temperature even in an oxidizing environment, and highly toxic.[10] Therefore, perovskite oxide has received

(Received March 28, 2018; accepted August 23, 2018; published online September 28, 2018)

great attention in major energy conversion technologies due to its thermal stability, low toxicity and excellent oxidation resistance.[11,12] The maximum power factor and the figure of merit in $SrTiO_3$[13,14] are found at large carrier concentrations of about 10^{21} cm^{-3} due to its large band gap of 3.2 eV, which are difficult to achieve in the bulk form but are accessible in thin films. In addition, it is possible to dope into a $SrTiO_3$ system with either electrons or holes in a controlled manner by elemental substitution as well as oxygen deficiency and excess,[15–19] allowing the enhancement of the thermoelectric performance. In the present work, the improvement of the thermoelectric properties of $SrTiO_3$ has been investigated by substitutional B-site doping with Cr.

EXPERIMENTAL

The substitutional B-site doped $SrTiO_3$ sample with Cr were prepared by a conventional solid-state reaction method. Appropriate amounts of raw materials including $SrCO_3$ (Sigma-Aldrich, – 325 mesh, 99.9%), TiO_2 (Sigma-Aldrich, – 325 mesh, 99.9%), and Cr_2O_3 (Sigma-Aldrich, – 325 mesh, 99.9%) were accurately weighted according to the stoichiometry and ball-milled in ethanol medium for 24 h. The slurry was dried at 80°C and ground to obtain powders. The powder was calcined at 1273 K for 6 h in air and then ground by ball milling in ethanol medium for 72 h to get fine powder for further use. The prepared powder was then pressed into pellets of diameter 10 mm by vacuum hot-pressing under a pressure of 70 MPa and sintered at 1573 K for 2 h. The pellets were cut into rectangular piece ($3 \times 3 \times 10$ mm^3) to measure the Seebeck coefficient and the electrical conductivity, and a cylindrical piece (10 mm × 1 mm) to measure the thermal conductivity, Hall coefficient and carrier concentration.

The phase characterization of the materials was performed by x-ray diffraction (Bruker D8 Advance system). The lattice parameter and the relative density of the materials were examined by a multiple peak-separation method and the Archimedes principle, respectively. The microstructure of the materials was characterized by a scanning electron microscope (SEM; FEI Quanta 400 system). The Hall coefficient, Hall mobility and carrier concentration were investigated by the van der Pauw method (Keithley 7065) at room temperature. The electrical conductivity and Seebeck coefficient were examined by the 4-probe methods (Ulvac-Rico, ZEM-3 system) from room temperature to 873 K in Ar atmosphere. $\kappa = \rho \times C_p \times d$ equation was used to calculate the thermal conductivity, where ρ is the density, C_p is the heat capacity (0.544 J/gK), and d is the thermal diffusivity. Thermal conductivity was examined by a laser flash method (Ulvac-Riko, TC-9000H) from room temperature to 873 K.

RESULTS AND DISCUSSION

The x-ray diffraction patterns for calcined and sintered $SrTi_{1-x}Cr_xO_3$ (x = 0.001, 0.002, 0.003, and 0.004) samples with standard $SrTiO_3$ (ICDD # 01-079-0174) are shown in Fig. 1a and b. From both Fig. 1a and b it is seen that the single phase of cubic perovskite structure was obtained comparing with the standard $SrTiO_3$ without any second phase. The [110] diffraction peak for Cr-doped $SrTiO_3$ with pure $SrTiO_3$ is illustrated in Fig. 1c. The peak shifted to a higher diffraction angle with increasing doping contents. The single-phase of cubic perovskite structure and the shifting of [110] diffraction peak with increasing doping contents clearly suggest that the substitutional doped $SrTiO_3$ with Cr was prepared with controlled doping levels.

Figure 2a demonstrates the lattice parameter of Cr-doped $SrTiO_3$ samples with a different doping level that was calculated by using a multiple peak-separation method. The lattice parameter increased with increasing doping contents, and this might be due to substitutional doping of small-sized Ti^{4+} ions (60.5 pm) with relatively large-sized Cr^{3+} ions Cr^{3+} ions (61.5 pm).[20] Figure 2b illustrates the relative density of all the disk samples of Cr-doped $SrTiO_3$ with a different doping level. The density varied from 99.59 to 99.80%. The density increases with increasing doping level up to x = 0.002 mol and then with increasing further doping level the density decreased. In this research, the $SrTi_{0.998}Cr_{0.002}O_3$ sample showed the highest density of 5.10 g/cm^3.

The microstructure of the $SrTi_{1-x}Cr_xO_3$ (x = 0.001, 0.002, 0.003, and 0.004) samples is shown in Fig. 3a, b, c and d. The average grain size is approximately 2.55, 2.70, 3.15, and 3.75 μm for x = 0.001, 0.002, 0.003, and 0.004 mol, respectively. The average grain size seems to be slightly increased by the incorporation of Cr_2O_3 into $SrTiO_3$ and these changes that occurred might be due to substitutional doping of small-sized Ti^{4+} ions (60.5 pm) with relatively large-sized Cr^{3+} ions Cr^{3+} ions (61.5 pm).[20] The changes of average grain size suggest that the microstructure of $SrTiO_3$ materials could be influenced by substitutional doping with Cr.

Initially in our research, we are trying to create excessive holes by Cr doping to produce p-type $SrTiO_3$ materials. However, p-type conduction was not shown in the series of experiments. Instead, we found enhanced TE properties from this set of experiments. The enhanced TE properties could be obtained possibly due to increase in the carrier concentration. Though Cr is an acceptor dopant, the carrier concentration might be increased by the oxygen vacancies that could be caused during the vacuum hot pressing. The temperature dependence of the thermoelectric properties such as Seebeck coefficient, electrical conductivity, thermal conductivity, and lattice thermal conductivity of $SrTi_{1-x}Cr_xO_3$ samples is shown in Fig. 4a, b, c and d. The temperature dependence of the Seebeck

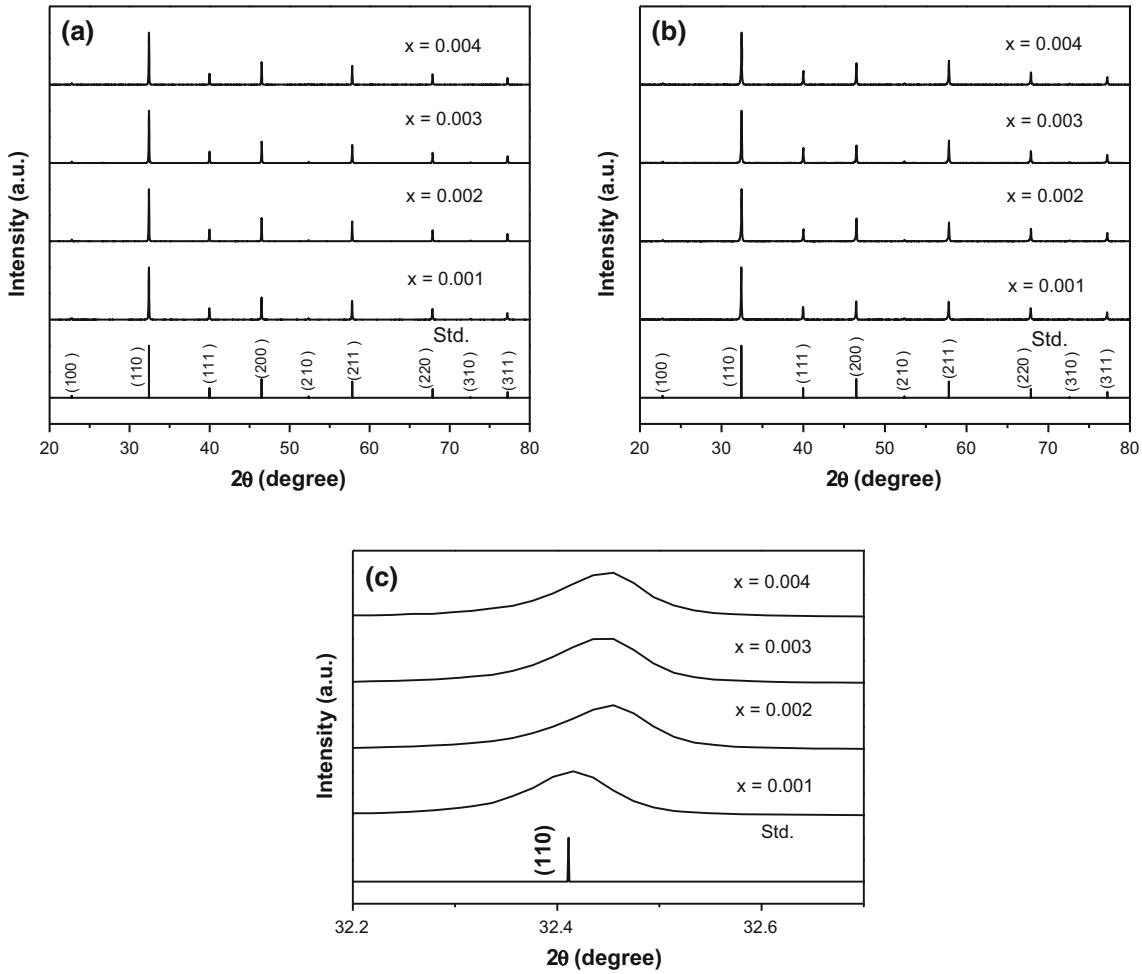

Fig. 1. X-ray diffraction patterns of $SrTi_{1-x}Cr_xO_3$ samples, (a) calcined powder, (b) vacuum hot pressed, and (c) [110] diffraction peak for Cr-doped $SrTiO_3$ with pure $SrTiO_3$.

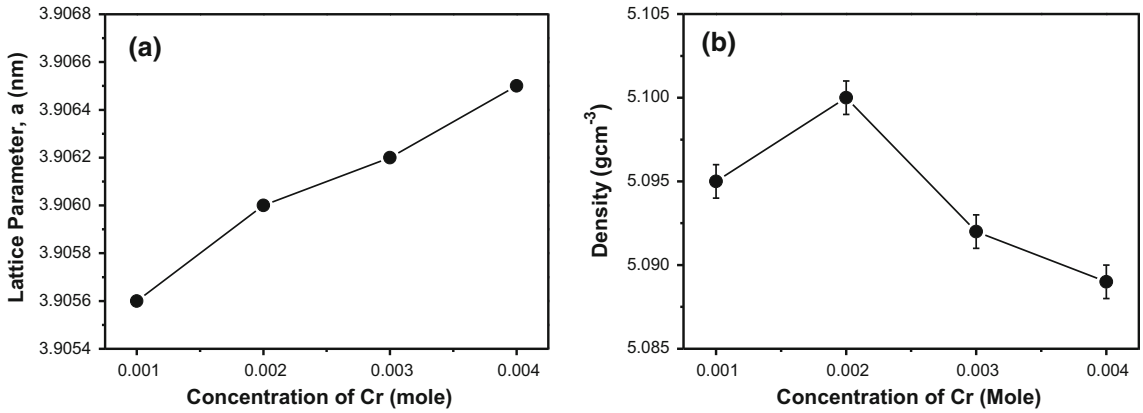

Fig. 2. (a) Lattice parameter as a function of the Cr content, and (b) density of $SrTi_{1-x}Cr_xO_3$ samples sintered at 1573 K. (a) $x = 0.001$, (b) $x = 0.002$, (c) $x = 0.003$, (d) $x = 0.004$.

coefficient of $SrTi_{1-x}Cr_xO_3$ samples is shown in Fig. 4a. In this research, the negative values of Seebeck coefficient, as well as the Hall coefficient of all the studied samples in the experimental temperature regime are confirming that the materials are an *n-type* conductor and electrons are the major carriers. Generally, the Seebeck coefficient of the thermoelectric material is expressed by Eq. 1.[21]

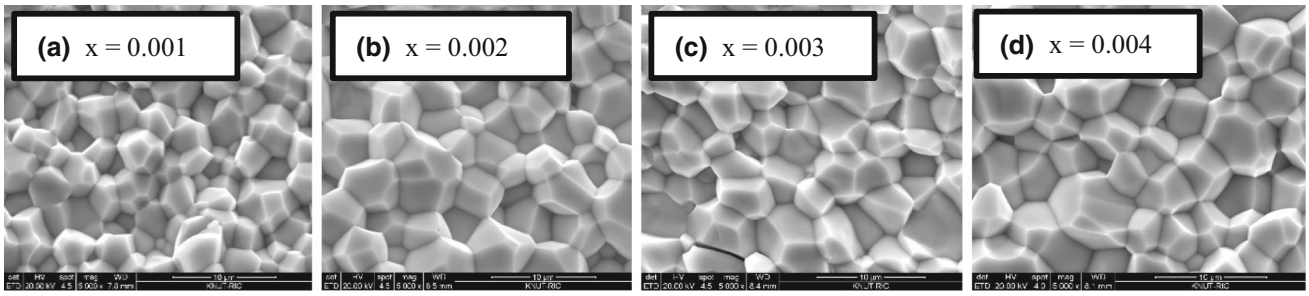

Fig. 3. SEM microstructure of $SrTi_{1-x}Cr_xO_3$ samples (a) x = 0.001 mol, (b) x = 0.002 mol, (c) x = 0.003 mol, and (d) x = 0.004 mol.

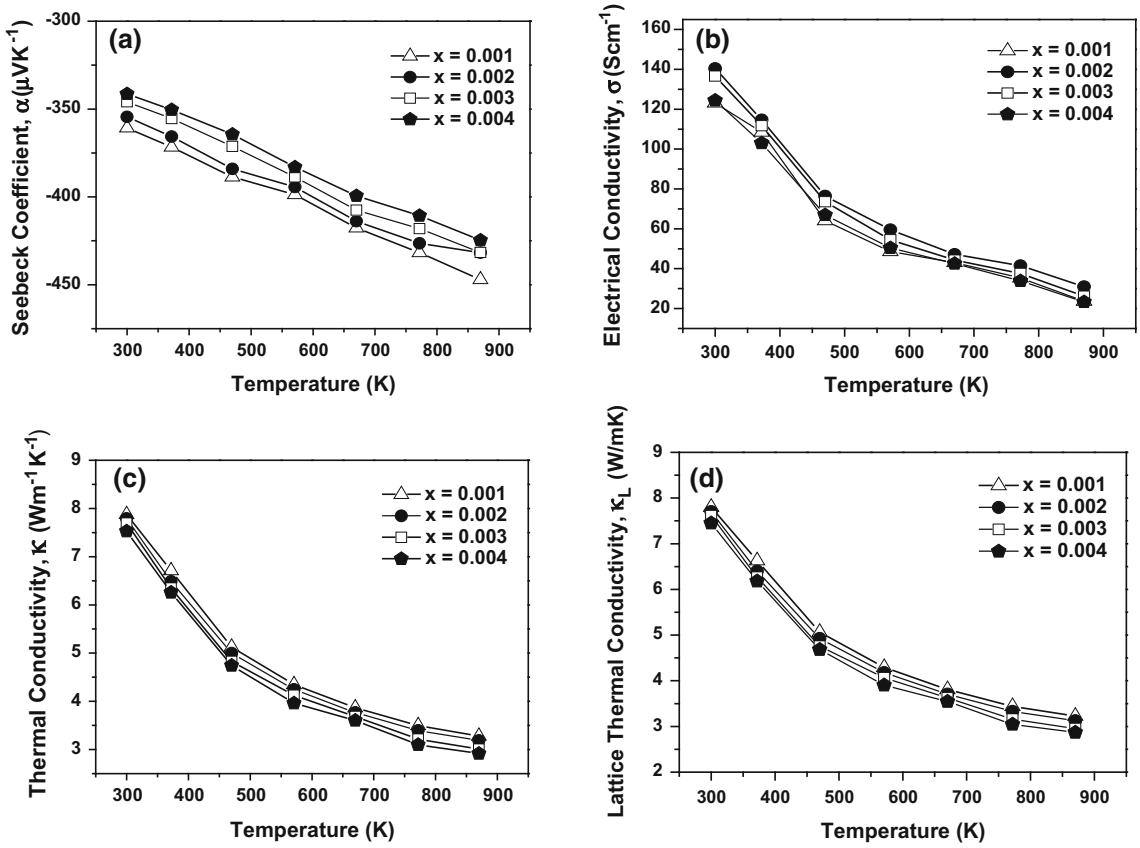

Fig. 4. Temperature dependence TE properties of $SrTi_{1-x}Cr_xO_3$ samples: (a) Seebeck coefficient, (b) electrical conductivity, (c) thermal conductivity, and (d) lattice thermal conductivity.

Table I. Electronic transport properties in terms of Hall coefficient, Hall mobility and carrier concentration of Cr-doped $SrTiO_3$ samples at room temperature

Composition (mol)	Hall coefficient ($cm^3\ C^{-1}$)	Hall mobility (μ, $cm^2\ V^{-1}\ s^{-1}$)	Carrier concentration (n, cm^{-3})
x = 0.001	− 2.050	853.00	1.52×10^{19}
x = 0.002	− 1.562	768.04	3.48×10^{19}
x = 0.003	− 0.851	312.79	6.53×10^{19}
x = 0.004	− 0.492	102.06	9.29×10^{19}

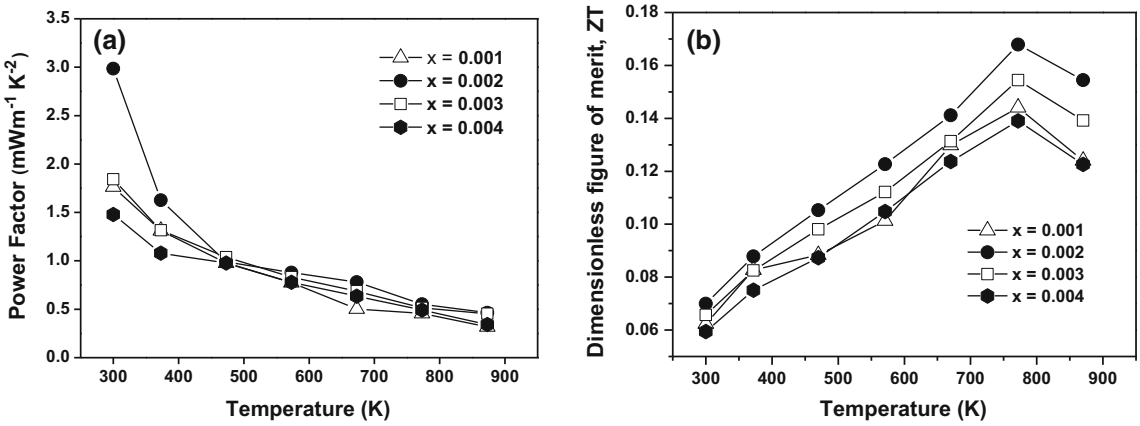

Fig. 5. Temperature dependence (a) power factor, and (b) ZT value of $SrTi_{1-x}Cr_xO_3$ samples.

$$S = \frac{8\pi^2 k_B^2 m^* T}{3eh^2}\left(\frac{\pi}{3n}\right)^{2/3}, \quad (1)$$

where k_B, e, h, T, m^*, and n is the Boltzmann's constant, electronic charge, the Planck's constant, temperature, effective mass of the carrier, and the carrier concentration. Equation 1 suggests that, the Seebeck coefficient is directly proportional to the effective mass and the inversely proportional to the carrier concentration at a given temperature. In this study, the absolute value of the Seebeck coefficient decreased with increasing Cr contents due to the fact that the carrier concentration increased with increasing Cr contents (as shown in Table I). Even though Cr is an acceptor dopant, the increasing behavior of carrier concentration is believed to cause the oxygen vacancies that could be created in the vacuum hot pressing. The maximum absolute value of the Seebeck coefficient was observed for $x = 0.001$ mol of Cr contents. The pristine (un-doped $SrTiO_3$) sample shows very low absolute value of the Seebeck coefficient that was reported by Mahmud et al.[22]

The temperature dependence of the electrical conductivity of $SrTi_{1-x}Cr_xO_3$ samples is shown in Fig. 4b. The electrical conductivity decreased with increasing temperature for all the studied Cr-doped $SrTiO_3$ samples in the experimental temperature regime, due to the degenerating behavior. In this study, the electrical conductivity increased with increasing doping level of Cr up to $x = 0.002$ mol due to a higher carrier concentration. Though high carrier concentration was observed with a doping level of $x > 0.002$ mol the electrical conductivity decreased because of low Hall mobility (as shown in Table I). The Hall mobility decreased with increasing Cr contents because of increasing the effective mass. The electrical conductivity of $SrTi_{1-x}Cr_xO_3$ samples is higher than that of pure $SrTiO_3$ because the carrier concentration of $SrTi_{1-x}Cr_xO_3$ samples increased because of the substitution of Ti^{4+} by Cr^{3+}. Similar behavior was observed in the report by Mahmud et al.[22]

The temperature dependence of the thermal conductivity and lattice thermal conductivity of $SrTi_{1-x}Cr_xO_3$ samples in the experimental temperature regime is shown in Fig. 4c and d. The thermal conductivity, κ, is defined by Wiedemann–Franz law and is given by $\kappa = \kappa_L + \kappa_E = \kappa_L + L_0\sigma T$ where κ_L is the lattice thermal conductivity by phonons, κ_E is the electronic thermal conductivity by carriers, and L_0 is a constant called Lorentz's number, and its value is 2.44×10^8 J^2 K^{-2} C^{-2}.[21] Figure 4d shows the temperature dependence of lattice thermal conductivity. The lattice thermal conductivity is 7.79 Wm^{-1} K^{-2} while the total thermal conductivity is 7.87 Wm^{-1} K^{-2} for $x = 0.001$ at room temperature. Therefore, lattice thermal conductivity plays a dominant role (approximately 98.98%) in the total thermal conductivity. In this study, the total thermal conductivity decreased with increasing temperature up to the experimental temperature regime. The decreasing behavior is believed to be caused by the decreased thermal diffusivity.[23] The total thermal conductivity observed in this study is also shown to be quite similar to the work by Shang et al.[24] and Otha et al.[25] and significantly smaller than that of single crystalline $SrTiO_3$.[26] It was also reported by Mahmud et al.[22] that, the un-doped $SrTiO_3$ shows relatively high thermal conductivity compare to our Cr-doped $SrTiO_3$. In this experiment, inconsistency in electron concentration, Hall mobility and electrical conductivity is hardly found, presumably due to the limited amount of doping (due to the limited solubility), and carrier concentration variation which could be caused during the vacuum hot consolidation process.

The temperature dependence of power factor, and ZT value for the $SrTi_{1-x}Cr_xO_3$ samples are shown in Fig. 5a and b. Figure 5a shows that, the power factor increased with increasing Cr contents up to $x = 0.002$ mol due to increasing electrical conductivity then decreased with further increasing of Cr

contents. From Fig. 5b, it is clearly seen that, for all doping levels, ZT increased with increasing temperature up to 773 K and reaches the maximum values of 0.144, 0.168, 0.154, and 0.139 for $x = 0.001$, 0.002, 0.003, and 0.004 mol of Cr-doped samples, respectively. The maximum value of ZT is observed due to the increased Seebeck coefficient with low thermal conductivity by the substitutional doping with Cr. The observed ZT value in this study suggests that the thermoelectric performance of $SrTiO_3$ can be influenced by the incorporation of Cr content.

CONCLUSIONS

The effect of B-site doping with Cr on the thermoelectric performance of the perovskite $SrTiO_3$ has been examined in this study. The B-site doped $SrTiO_3$ with Cr was synthesized by a conventional solid-state reaction method followed by vacuum hot-pressing. Structural characterization was evaluated by XRD and SEM. Electronic and thermal transport properties were examined to determine the thermoelectric properties of the samples. The doping on the B-site of the perovskite oxide with Cr plays a significant role to enhance the Seebeck coefficient and reducing the thermal conductivity, and, hence, improving the ZT. The thermal conductivity decreased with increasing doping level through our experimental doping range but the thermoelectric power factor increased with doping level up to $x = 0.002$ mol due to the large value of Seebeck coefficient and electrical conductivity. The maximum dimensionless figure of merit was obtained for $SrTi_{0.998}Cr_{0.002}O_3$ samples with a relatively high value of power factor and significantly low value of thermal conductivity. In this research, the maximum value of the figure of merit, ZT = 0.168 at 773 K was observed for the $SrTi_{0.998}Cr_{0.002}O_3$ sample.

ACKNOWLEDGEMENTS

This work was supported by a Grant from the Regional Innovation Center (RIC) Program, which was conducted by the Ministry of SMEs and Startpus of the Korean Government.

REFERENCES

1. S. Shafiee and R.A. Salim, *Energy Policy* 66, 547 (2014).
2. S. Shafiee and E. Topal, *Energy Policy* 37, 181 (2009).
3. J.R. Sootsman, D.Y. Chung, and M.G. Kanatzidis, *Angew. Chem. Int.* 48, 8616 (2009).
4. J.-F. Li, W.S. Liu, L.D. Zhao, and M. Zhou, *NPG Asia Mater.* 2, 152 (2010).
5. F. Casper, T. Graf, S. Chadov, B. Balke, and C. Felser, *Semi-cond. Sci. Technol.* 27, 3 (2012).
6. D.-Y. Chung, T. Hogan, P. Brazis, M. Rocci-Lane, C. Kannewurf, M. Bastea, C. Uher, and M.G. Kanatzidis, *Science* 287, 1024 (2000).
7. B.C. Sales, D. Mandrus, and R.K. Williams, *Science* 272, 1325 (1996).
8. R.T. Littleton IV, T.M. Tritt, J.W. Kolis, and D.R. Ketchum, *Phys. Rev. B Condens. Matter* 60, 13453 (1999).
9. C. Yu, T. Zhu, R. Shi, Y. Zhang, X. Zhao, and J. He, *Acta Mater.* 57, 2757 (2009).
10. I. Terasaki, Y. Sasago, and K. Uchinokura, *Phys. Rev. B Condens. Matter* 56, R12685 (1997).
11. A. Weidenkaff, R. Robert, M.H. Aguirre, L. Bocher, T. Lippert, and S. Canulescu, *Renew. Energy* 33, 342 (2008).
12. P. Tomes, R. Robert, M. Trottmann, L. Bocher, M.H. Aguirre, J. Hejtmanek, and A. Weidenkaff, *J. Electron. Mater.* 39, 1696 (2010).
13. H. Ohta, S. Kim, Y. Mune, T. Mizoguchi, K. Nomura, S. Ohta, T. Nomura, Y. Nakanishi, Y. Ikuhara, M. Hirano, H. Hosono, and K. Koumoto, *Nat. Mater.* 6, 129 (2007).
14. K. Koumoto, Y. Wang, R. Zhang, A. Kosuga, and R. Funahashi, *Annu. Rev. Mater. Res.* 40, 363 (2010).
15. S.Y. Watanebe, J.G. Bednorz, A. Bietsch, C. Gerber, D. Widmer, A. Beck, and S.J. Wind, *J. Wind Appl. Phys. Lett.* 78, 3738 (2001).
16. J. Inaba and T. Katsufuji, *Phys. Rev. B Condens. Matter Mater. Phys.* 72, 054208 (2005).
17. T. Hara, *Mater. Chem. Phys.* 91, 243 (2005).
18. T.H. Fang, Y.J. Hsiao, Y.S. Chang, and Y.H. Chang, *Mater. Chem. Phys.* 100, 418 (2006).
19. A. Tkach, P.M. Vilarinho, A.L. Kholkin, A. Paskhin, S. Veljko, and J. Petzelt, *Phys. Rev. B Condens. Matter Mater. Phys.* 73, 104113 (2006).
20. R.D. Shannon, *Acta Crystallogr. A* A32, 751 (1976).
21. A. Willfahart, Screen Printed Thermoelectric Devices, Linkopings University, SE-601, 74, (2014).
22. I. Mahmud, M.-S. Yoon, I.-H. Kim, M.-K. Choi, and S.-C. Ur, *J. Korean Phys. Soc.* 68, 35 (2016).
23. P.-P. Shang, B.-P. Zhang, Y. Liu, J.-F. Li, and H.-M. Zhu, *J. Electron. Mater.* 40, 926 (2011).
24. P.-P. Shang, B.-P. Zhang, J.-F. Li, and N. Ma, *Solid State Sci.* 12, 1341 (2010).
25. S. Ohta, T. Nomura, H. Ohta, M. Hirano, H. Hosono, and K. Koumoto, *Appl. Phys. Lett.* 87, 092108 (2005).
26. T. Okuda, K. Nakanishi, S. Miyasaka, and Y. Tokura, *Phys. Rev. B Condens. Matter Mater. Phys.* 63, 113104 (2001).